*Article*

# Photocatalytic Decolorization of Dye with Self-Dye-Sensitization under Fluorescent Light Irradiation

**Md. Ashraful Islam Molla [1,\*], Mai Furukawa [1], Ikki Tateishi [1], Hideyuki Katsumata [1], Tohru Suzuki [2] and Satoshi Kaneco [1,2]**

[1] Department of Chemistry for Materials, Graduate School of Engineering, Mie University, Tsu 514-8507, Japan; maif@chem.mie-u.ac.jp (M.F.); teishi@gmail.com (I.T.); hidek@chem.mie-u.ac.jp (H.K.); kaneco@chem.mie-u.ac.jp (S.K.)

[2] Mie Global Environment Center for Education & Research, Mie University, Tsu 514-8507, Japan; suzuki@chem.mie-u.ac.jp

\* Correspondence: professoraislam@gmail.com; Tel.: +81-59-231-9427

**Abstract:** A dye-sensitization technique was applied to effective catalysts—$TiO_2$ and ZnO—under fluorescent light irradiation for Orange II (OII) and Methyl Orange (MO) degradations. Treatments were carried out at different time periods using 20 mg of catalysts and 30 mL of 5 mg/L of OII and MO. The degradation efficiency of OII and MO increased with increasing irradiation time under irradiation of fluorescent light. The photocatalytic activity of ZnO nanoparticles was better compared with that of $TiO_2$ for MO; and the ZnO activity was the same as $TiO_2$ for OII photodegradation. Kinetic behavior was evaluated in terms of the Langmuir–Hinshelwood model (pseudo-first order kinetic). The possible mechanism of photodegradation under fluorescent light was discussed.

**Keywords:** photocatalytic degradation; fluorescent light; self-dye-sensitization; ZnO; $TiO_2$

## 1. Introduction

Titanium dioxide ($TiO_2$) and zinc oxide (ZnO) have drawn great attention, because they have become one of the most effective photocatalysts in the mineralization of toxic organic substances, owing their virtues of low cost, highly chemical stability, and nontoxicity [1,2]. However, these catalysts can only be excited by the irradiation of UV light, due to their wide band gaps. An artificial light source, for instance an Hg-Xe lamp, is particularly expensive, whereas a fluorescent lamp is cheap, has a longer life time, and uses less energy. The UV region occupies only a small fraction of a fluorescent lamp's spectrum. This problem can be solved only by improving the light absorption capacity of photocatalysts [3,4]. Photocatalysts can be modified in order to expand their photoresponse to the visible region for pollutant degradation with several ways, including the doping with cations/anions or the coupling with another small band gap materials [5]. Most of these methods, however, are time-consuming and quite expensive. Dye sensitization, on the other hand, is a simpler method that can extend catalysts activation to longer wavelengths compared with those corresponding to its band gap. Dye sensitization begins with electron injection into the conduction band (CB) of a photocatalyst from the excited dye, followed by interfacial electron transfer [6,7].

Recently, the self-sensitized degradation of dye under visible light irradiation has been investigated. Wu et al. [8] studied self-photosensitized oxidative decolorization of rhodamine B under visible light irradiation in $TiO_2$ dispersions with a halogen lamp and cutoff filter. The photosensitized degradation of a textile azo dye with $TiO_2$ using visible light with a fiber optic illuminator was reported by Vinodgopal and Kamat [9]. Xing et al. [10] studied the enhanced self-sensitized degradation of

colored pollutants under visible light with a mercury lamp and filter. The photocatalytic performance of ZnO for self-sensitized degradation of malachite green under solar light was investigated by Saikia et al. [11]. According to our knowledge, there is little information on the photocatalytic decolorization of dye in water with self-dye-sensitized photocatalysts under room fluorescent light irradiation with very weak intensity.

The present work deals with photocatalytic decolorization of dye in water with self-dye-sensitized TiO$_2$ and ZnO under room fluorescent light irradiation.

## 2. Materials and Methods

### 2.1. Materials

All reagents were of analytical grade and were used without further treatment. Orange II and methyl orange used in this study were purchased from Nacalai Tesque Inc., Kyoto, Japan (grade >99%). TiO$_2$ powder (P25, purity 99.9%) was obtained from Degussa Co., Essen, Germany. ZnO was purchased from Sigma-Aldrich, St. Louis, MO, USA. Ultrapure water (18 M$\Omega$ cm) was prepared by an ultrapure water system (Advantec MFS Inc., Tokyo, Japan). The detailed experimental conditions were shown in Table 1.

**Table 1.** Experimental conditions.

| | |
|---|---|
| Samples | Orange II (5 mg/L, 30 mL) <br> Methyl orange (5 mg/L, 30 mL) |
| Photocatalyst | P25 TiO$_2$ (20 mg) <br> Aldrich ZnO (20 mg) |
| Temperature | Room temperature (25 °C) |
| pH | 6 |
| Light source | 450 nm LED light (5.14 mW/cm$^2$) <br> Fluorescent light (0.034 mW/cm$^2$) |
| $\lambda_{max}$ | Orange II (485 nm), methyl orange (464 nm) |
| Irradiation time | 6 h |

### 2.2. Characterization of Photocatalyst

In order to record the diffraction patterns of photocatalysts (TiO$_2$ and ZnO), the powder X-ray diffractometer (XRD, RIGAKU Ultima IV, sample horizontal type) was used in the condition of Cu K$\alpha$ radiation of wavelength 0.15406 nm with tube current of 50 mA at 40 kV in 2θ angle range from 10° to 80° with a scan speed of 4°/min and a step size of 0.02°. Figure S1 shows the X-ray diffraction (XRD) pattern of TiO$_2$. Because P25 is a mixture of 20% rutile and 80% anatase, XRD pattern shows both anatase and rutile lines [12]. Figure S2 illustrates the XRD of ZnO. Three main distinct peaks at 31.76°, 34.42°, and 36.26° are observed in the patterns, which are indexed to the (100), (002), and (101) diffractions of the wurtzite ZnO, respectively [13]. The particle size of the TiO$_2$ and ZnO have been obtained from the full width at half maximum (FWHM) of the most intense peaks of the respective crystals using the Scherrer equation, $D = 0.9\lambda/\beta\cos\theta$, where $\lambda$ is the X-ray wavelength, $D$ the average crystallite size, $\theta$ the Bragg diffraction angle, and $\beta$ the full width at half-maximum. The crystal size of TiO$_2$ and ZnO could be estimated as ~21 and ~38 nm, respectively.

The diffuse reflectance spectra (DRS) of photocatalysts were checked over a range of 200–800 nm using a Shimadzu UV-2450 UV–vis system equipped with an integrating sphere diffuse reflectance accessory with the reference material BaSO$_4$. The diffuse reflectance spectra of the TiO$_2$ and ZnO samples were studied, as shown in Figures S3 and S4. The reflectance data was converted to Kubelka–Munk equation which is expressed as $F(R) = (1 - R)^2/2R$. The optical band gap of TiO$_2$ was deduced by extrapolating the straight linear portion of the plot of $[F(R)hv]^{0.5}$ versus the photon energy

(*hv*) to the phonon energy axis, which is shown in the interior of Figure S3. The band gap of ZnO was estimated from the Tauc plot of $[F(R)hv]^2$ versus photon energy, which is presented in the interior of Figure S4.

## 2.3. Evaluation of Photocatalytic Activity

The photodegradation system is illustrated in Figure S5. The photocatalytic activities of $TiO_2$ and ZnO were checked by the decolorization of two typical azo dyes, orange II (OII) and methyl orange (MO), under 450 nm LED light and fluorescent light irradiation. The photocatalytic reactions were performed in a Pyrex glass reactor. The catalyst powder (20 mg) was suspended in 30 mL of dye solutions with 5 mg/L without adjustment of pH. The luminous intensities were measured by a LI-COR light sensor (LI-250A), and were 5.1 mW/cm$^2$ for LED lamp and 0.034 mW/cm$^2$ for fluorescent light, respectively. The adsorption experiment was conducted with aluminum foil coverage to block the impact of radiation. Prior to light illumination, the catalyst suspension was dispersed by a magnetic stirrer for 30 min in the dark, to achieve adsorption equilibrium. During irradiation, the catalyst was kept in suspension state by a magnetic stirrer. After the illumination, the catalyst was separated through the Advantec membrane filter 0.45 μm. The catalysts could be almost removed by the filtration. The concentration of dye was measured using a UV–visible spectrometry (UV-1650PC, SHIMADZU Co., Tokyo, Japan). According to Beer–Lambert law, the relative concentration ($C/C_0$) of the OII solution was calculated by the relative absorbance ($A/A_0$) at 485 nm, where $A_0$ and $A$ are the absorbance of the OII solution at the beginning time ($t_0$) of photocatalytic treatment and at time $t$, respectively. The photodegradation of OII under fluorescent light irradiation was similar to that under visible light irradiation except for the light source. The photodegradation of MO (5 mg/L) was similar to that of OII except that the detection wavelength was 464 nm.

## 3. Results and Discussion

### 3.1. UV–Visible Analysis

The temporal absorption spectral changes during the photocatalytic decolorization of OII and MO with $TiO_2$ and ZnO under fluorescent and 450 nm light illuminations were investigated, as shown in Figures 1 and 2, respectively. As they can be seen, the intensities of the peak at 485 and 464 nm progressively decreased with increasing irradiation time up to 360 min. The well-defined absorption bands decreased after irradiation for 360 min, indicating that OII and MO had been decolored in the presence of $TiO_2$ and ZnO with fluorescent light and 450 nm LED light irradiation. Therefore, the self-dye-sensitization was very effective for the decolorization of OII and MO under fluorescent and 450 nm light illuminations.
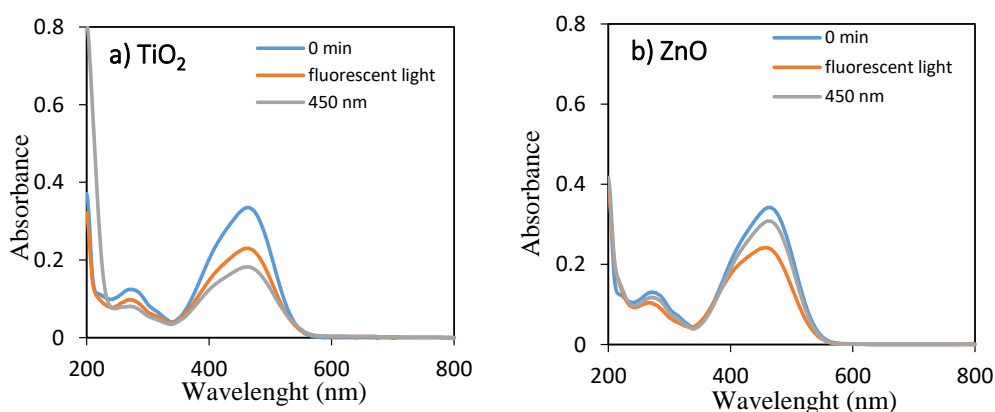


**Figure 1.** UV–visible spectra of aqueous solutions of OII for 0 min and 360 min using (**a**) $TiO_2$ and (**b**) ZnO under fluorescent and 450 nm LED lights.
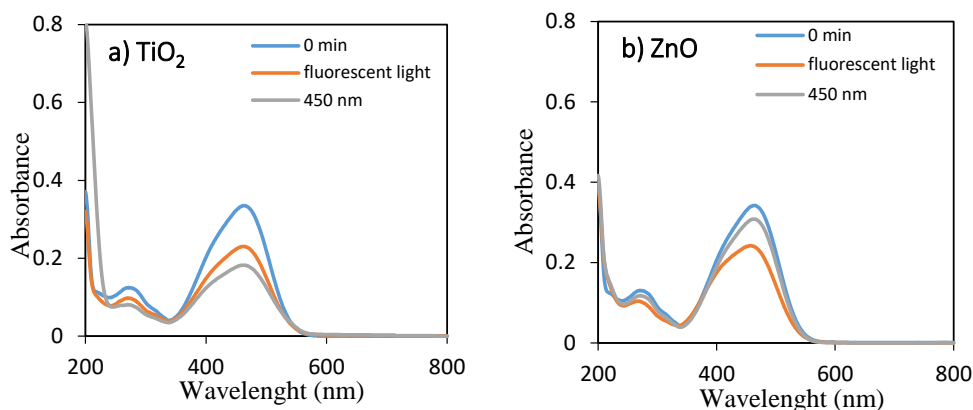
**Figure 2.** UV–visible spectra of aqueous solutions of MO for 0 min and 360 min using (**a**) TiO$_2$ and (**b**) ZnO under fluorescent and LED lights.

### 3.2. Photocatalytic Decolorization of OII and MO with TiO$_2$

The effect of irradiation time on photocatalytic decolorization of dye (OII and MO) was performed by measuring the percentage of dye removal at different periods under fluorescent and 450 nm LED lights, as shown in Figure 3a,b, respectively. The percentage of OII and MO removal increased with an increase in irradiation time, and reached up to about 61% and 24% for fluorescent light and about 88% and 41% for LED light after 6 h, respectively. The adsorption (removal) percentage of OII on TiO$_2$ particles was large up to 30 min, whereas MO adsorption was very little. There was little change in the OII and MO solutions during photolysis. The photocatalytic decolorization processes of both dyes under LED light were more effective compared with those obtained under fluorescent light radiation. These facts may be due to the light intensity, because the amounts of electron–hole pairs are dependent on them [14].
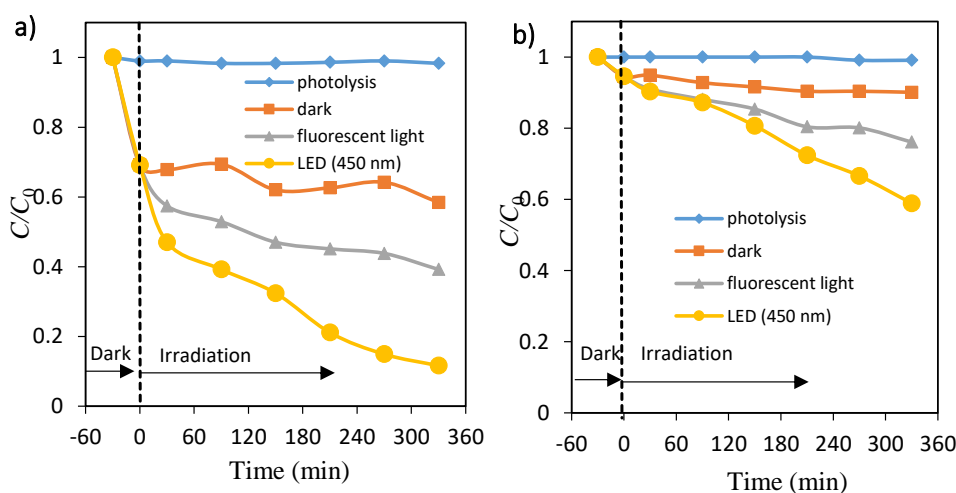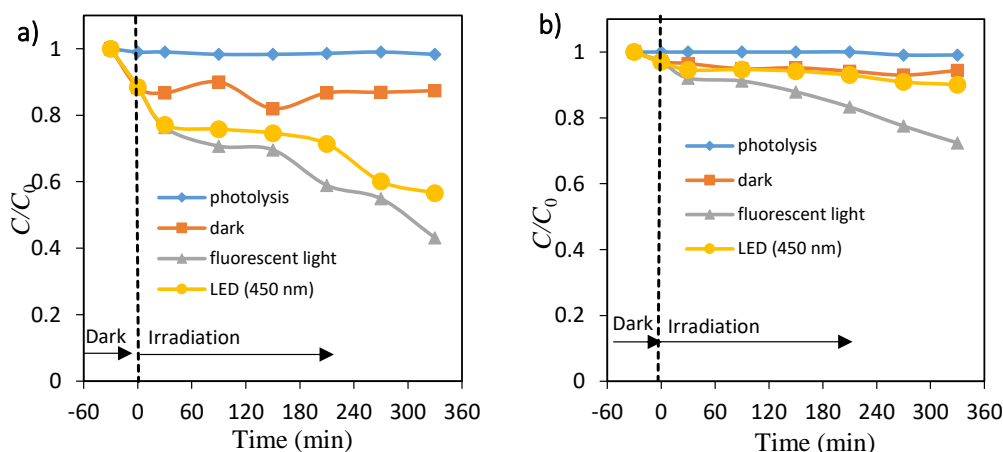


**Figure 3.** Time courses of concentration of orange II (**a**) and methyl orange (**b**). Photolysis: ◆, TiO$_2$ dispersions: under dark ■, under fluorescent light irradiation ▲ and under LED light irradiation ●.

### 3.3. Photocatalytic Decolorization of OII and MO with ZnO

Figure 4a,b shows the percentage of dye (OII and MO) in the presence of ZnO nanopowders under fluorescent light and 450 nm LED light. About 57% and 28% degradation of OII and MO took place at 6 h under fluorescent light, whereas about 43% and 10% was eliminated under 450 nm LED light. Negligible decolorization occurred in the presence of fluorescent light and 450 nm LED light without any catalyst, as shown in Figure S6a,b. Without the presence of either photocatalysts (TiO$_2$ and ZnO)

or the light (fluorescent and 450 nm) radiation, little change in the absorbance values was observed. The adsorption (removal) percentage of OII on $TiO_2$ and ZnO particles was large, whereas adsorption of MO on the same photocatalyst was very little in the time range. This weaker adsorption process of methyl orange compared to the OII dye could be due to the MO molecule having only one $SO_3^-$ group while the OII molecule has one $SO_3^-$ and one OH group. These observations reveal that visible light and a photocatalyst are needed for effective decolorization of dye.



**Figure 4.** Time courses of concentration of orange II (**a**) and methyl orange (**b**). Photolysis: ♦, ZnO dispersions: under dark ■, under fluorescent light irradiation ▲ and under LED light irradiation ●.

### 3.4. Kinetic Analysis

The photocatalytic oxidation process for many organic contaminants has often been modeled with the Langmuir–Hinshelwood (L–H) equation, which also covers the adsorption properties of the substrate on the photocatalyst surface. This model was developed by Turchi and Ollis [15] and expressed as Equation (1):

$$r_0 = -\frac{dC}{dt} = \frac{kKC}{1+KC} \tag{1}$$

where $r_0$ is the degradation rate of the reactant, $k$ is the reaction rate constant, and $K$ and $C$ are the adsorption equilibrium constant and concentration for the reactant, respectively. If the concentration of reactant is very low, i.e., $KC << 1$, the L–H equation (Equation (1)) simplifies to a pseudo-first-order kinetic law (Equation (2)) where $k_{obs}$ is being the apparent pseudo-first-order rate constant.

$$-\frac{dC}{dt} = kKC = k_{obs}C \tag{2}$$

Integration of the above equation with the limit of $C = C_0$ at $t = 0$ with $C_0$ gives the equation:

$$-\mathrm{Ln}\frac{C}{C_0} = k_{obs}t \tag{3}$$

The primary degradation reaction is estimated to follow a pseudo first-order kinetic law, according to Equation (3). In order to confirm the speculation, $\mathrm{Ln}(C/C_0)$ was replotted as a function of illumination time for OII and MO shown in Figures 5 and 6, respectively. Because the linear plots were observed as expected, the kinetics of OII and MO in the $TiO_2$ suspension solution followed the first-order degradation curve, which agreed with the L–H model resulting from the low coverage in the experimental concentration range (5 mg/L).
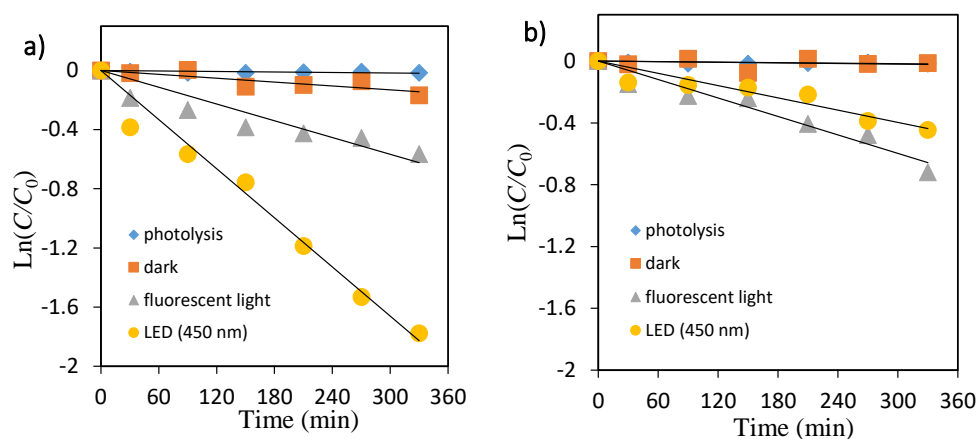
**Figure 5.** Kinetic plot of Ln($C/C_0$) versus irradiation time for the photocatalytic degradation of orange II. (**a**) $TiO_2$, (**b**) ZnO.
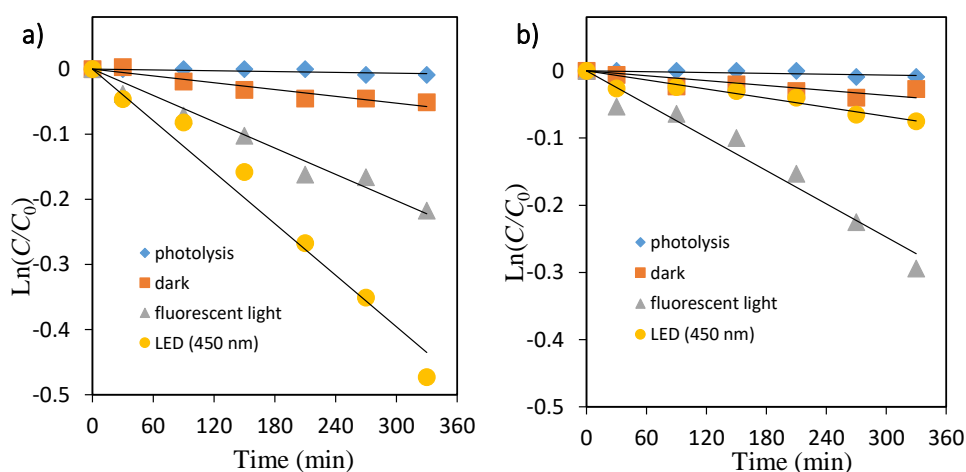


**Figure 6.** Kinetic plot of Ln($C/C_0$) versus irradiation time for the photocatalytic degradation of methyl orange. (**a**) $TiO_2$, (**b**) ZnO.

The photocatalytic decolorization kinetic parameters such as pseudo-first-order rate constant, correlation coefficient, and substrate half-life are shown in Table 2. The values of rate constants have been determined from the slope of these plots. As shown in Table 2, the rate constant values $k_{obs}$ (min$^{-1}$) were lower in fluorescent light compared with that under LED light for both dyes.

**Table 2.** Rate constants, $R^2$, and half-life values of OII and MO dyes using $TiO_2$ and ZnO.

| Light Source | Catalysts | $k_{obs}$ (min$^{-1}$) | | $R^2$ | | $t_{1/2}$ (min) | |
|---|---|---|---|---|---|---|---|
| | | OII | MO | OII | MO | OII | MO |
| Fluorescent light | $TiO_2$ | 0.0019 | 0.00067 | 0.80 | 0.97 | 367 | 1029 |
| | ZnO | 0.0019 | 0.00083 | 0.93 | 0.96 | 346 | 866 |
| LED light | $TiO_2$ | 0.0055 | 0.0013 | 0.97 | 0.98 | 125 | 525 |
| | ZnO | 0.0013 | 0.00023 | 0.88 | 0.88 | 533 | 3465 |

### 3.5. Proposed Degradation Mechanisms

$TiO_2$ and ZnO cannot absorb visible light energy directly due to the band gap 3.2 eV (Supplementary Data Figures S3 and S4) [16]. On the contrary, when a colored organic compound

is present, a sensitized photocatalytic process is possible. Huang et al. investigated dye sensitized photodegradation which follows the radical mechanism [17]. Molla et al. recently evaluated the reaction mechanism of photocatalytic degradation of dye with self-sensitized $TiO_2$ under visible light [18]. Park et al. also mentioned that the dye-sensitization can be applied for the self-degradation of dyes. In dye-sensitization, a dye absorbing visible light excites an electron from the HOMO (highest occupied molecular orbital) of a dye to the LUMO (lowest unoccupied molecular orbital) [19]. The HOMO and LUMO levels and band gap energy of OII and MO were obtained from literature and the values are presented in Table 3.

**Table 3.** HOMO and LUMO levels and energy gaps (eV) of dye molecules and $\lambda_{max}$ (nm).

| Molecules | HOMO | LUMO | Energy Gaps | $\lambda_{max}$ | Reference |
|-----------|------|------|-------------|-----------------|-----------|
| OII | 0.17 | −1.86 | 2.03 | 485 | [20] |
| MO | 0.84 | −2.43 | 3.27 | 464 | [21] |

Figure 7 demonstrates the valence band (VB) and conduction band (CB) levels and the energy gaps of catalyst vs. NHE reference electrodes. It is observed that the LUMO levels of OII and MO are more negative relative to the conduction band edge potential of $TiO_2$ and ZnO. Otherwise, due to the more negative potential of the lowest unoccupied molecular orbital (LUMO) level for dye relative to the conduction band (CB) of the catalyst [22], the electron transfer from the LUMO of dyes to the CB of the catalyst is feasible. It is reported that the redox potential of $O_2/{}^{\bullet}O_2{}^-$ is −0.33 V vs. NHE [23], which is more positive than conduction band potential of $TiO_2$ and ZnO (−0.5 V vs. NHE) [24,25].
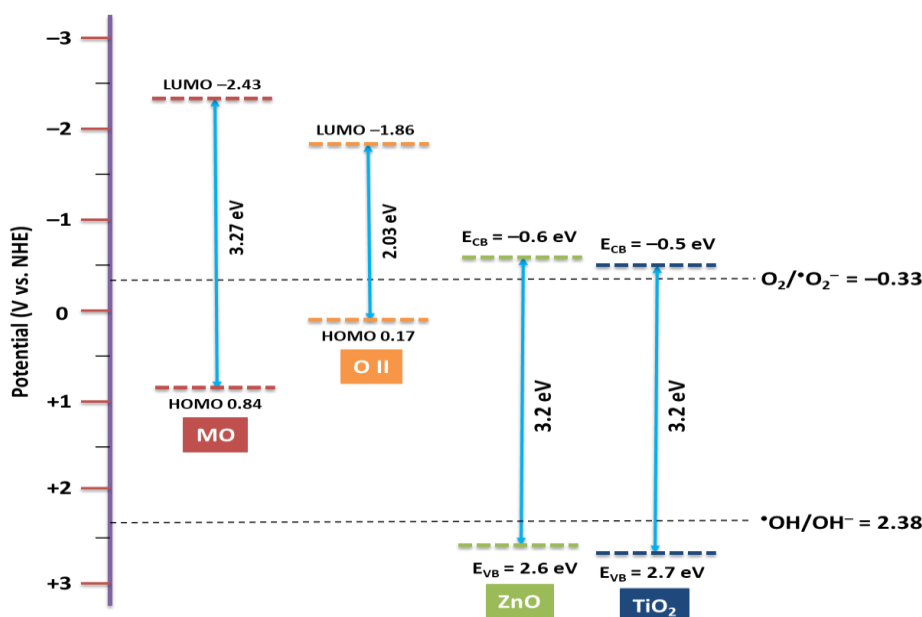


**Figure 7.** Schematic energy level diagram of $TiO_2$ and ZnO with respect to potential of $O_2/{}^{\bullet}O_2{}^-$ and ${}^{\bullet}OH/OH^-$ and the HOMO–LUMO levels of dye.

The surface adsorbed dyes were excited by absorbing visible light (fluorescent) and donated their electrons to the conduction band of the catalyst. As a result, the dyes are converted to a cationic radical (dye$^{+\bullet}$), and ${}^{\bullet}O_2{}^-$ radical specie were easily formed by the adsorbed oxygen through capturing electrons from the conduction band of the catalyst. The ${}^{\bullet}O_2{}^-$ can react with surface adsorbed $H_2O$ to form $H_2O_2$ which is ultimately converted to ${}^{\bullet}OH$ [26,27]. The surface adsorbed OII and MO radical cation or surface adsorbed dyes can undergo degradation by ${}^{\bullet}O_2{}^-$ and ${}^{\bullet}OH$. As soon as a dye molecule degrades, another dye molecule will be adsorbed on $TiO_2$ and ZnO surface and the photocatalytic

cycle continues. The peak corresponding to the azo group of dye (OII and MO) decreased after 360 min of irradiation (Figure 1a,b and Figure 2a,b). This may be attributed to the fact that azo bonds are more reactive than the aromatic part of the molecule. They are easily oxidized by the photogenerated •OH radicals. The cleavage of the azo (–N=N–) bond leads to decolorization of dyes [28]. According to the previous studies, a possible decolorization pathway of OII [29] and MO [30] was proposed in Figure 8.
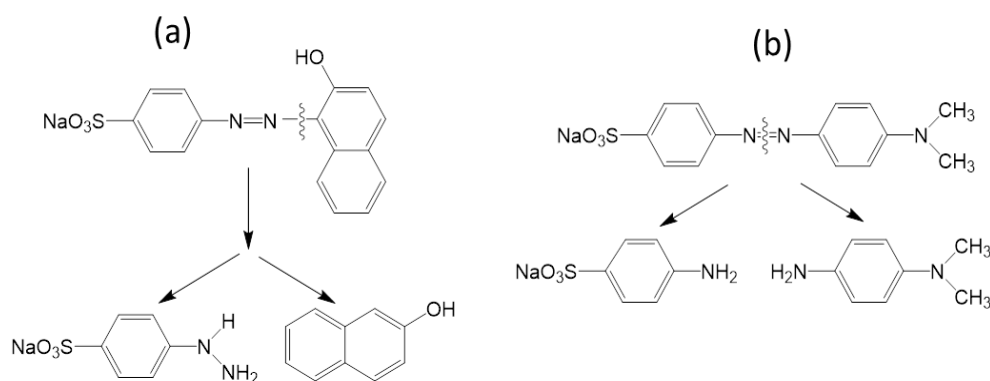


**Figure 8.** Proposed decolorization mechanism of OII (**a**) and MO (**b**) under visible light.

## 4. Conclusions

Consequently, the photocatalytic activity of self-dye-sensitized $TiO_2$ and ZnO in the degradation of OII and MO was studied under fluorescent light irradiation. The percentage of degradation of OII and MO increased with an increase in irradiation time under fluorescent light for $TiO_2$ and ZnO catalyst. The photocatalytic activity of ZnO nanoparticles was better than that of $TiO_2$ for MO, and of ZnO and $TiO_2$ showed the same activity for OII photodegradation under fluorescent light. The kinetics of OII and MO photodegradation followed the pseudo-first order rate law, and could be described in terms of the Langmuir–Hinshelwood model. The photocatalytic degradation of waste dye in water with self-dye-sensitized $TiO_2$ and ZnO under fluorescent light irradiation will become a promising technique.

## References

1. Ong, W.J.; Tan, L.L.; Chai, S.P.; Yong, S.T.; Mohamed, A.R. Highly reactive {001} facets of $TiO_2$-based composites: Synthesis, formation mechanism and characterization. *Nanoscale* **2014**, *6*, 1946–2008. [CrossRef] [PubMed]
2. Zhang, Q.; Dandeneau, C.S.; Zhou, X.; Cao, G. ZnO nanostructures for dye sensitized solar cells. *Adv. Mater.* **2009**, *21*, 4087–4108. [CrossRef]

3.   Ni, M.; Leung, M.K.H.; Leung, D.Y.C.; Sumathy, K. A review and recent developments in photocatalytic water-splitting using TiO$_2$ for hydrogen production. *Renew. Sustain. Energy Rev.* **2007**, *11*, 401–425. [CrossRef]

4.   Di Mauroa, A.; Cantarella, M.; Nicotra, G.; Privitera, V.; Impellizzeri, G. Low temperature atomic layer deposition of ZnO: Applications in photocatalysis. *Appl. Catal. B Environ.* **2016**, *196*, 68–76. [CrossRef]

5.   Impellizzeri, G.; Scuderi, V.; Romano, L.; Napolitani, E.; Sanz, R.; Carles, R.; Privitera, V. C ion–implanted TiO$_2$ thin film for photocatalytic applications. *J. Appl. Phys.* **2015**, *117*, 105308. [CrossRef]

6.   Kim, W.; Tachikawa, T.; Majima, T.; Choi, W. Photocatalysis of dye–sensitized TiO$_2$ nanoparticles with thin overcoat of Al$_2$O$_3$: Enhanced activity for H$_2$ production and dechlorination of CCl$_4$. *J. Phys. Chem. C* **2009**, *113*, 10603–10609. [CrossRef]

7.   Duncan, W.R.; Prezhdo, O.V. Theoretical studies of photoinduced electron transfer in dye-sensitized TiO$_2$. *Annu. Rev. Phys. Chem.* **2007**, *58*, 143–184. [CrossRef] [PubMed]

8.   Wu, T.; Liu, G.; Zhao, J.; Hidaka, H.; Serpone, N. Photoassisted degradation of dye pollutants. V. Self-photosensitized oxidative transformation of *rhodamine B* under visible light irradiation in aqueous TiO$_2$ dispersions. *J. Phys. Chem. B* **1998**, *102*, 5845–5851.

9.   Vinodgopal, D.; Kamat, P.V. Enhanced rates of photocatalytic degradation of an azo-dye using SnO$_2$/TiO$_2$ coupled semiconductor thin-films. *Environ. Sci. Technol.* **1995**, *29*, 841–845. [CrossRef] [PubMed]

10.  Xing, G.; Tang, C.; Zhang, B.; Zhao, L.; Su, Y.; Wang, X. A highly uniform ZnO/NaTaO$_3$ nanocomposite: Enhanced self-sensitized degradation of colored pollutants under visible light. *J. Alloy Compd.* **2015**, *647*, 287–294. [CrossRef]

11.  Saikia, L.; Bhuyan, D.; Saikia, M.; Malakar, B.; Dutta, D.K.; Sengupta, P. Photocatalytic performance of ZnO nanomaterials for self-sensitized degradation of malachite green dye under solar light. *Appl. Catal. A Gen.* **2015**, *490*, 42–49. [CrossRef]

12.  Selvam, K.; Swaminathan, M. Photocatalytic synthesis of 2-methylquinolines with TiO$_2$ Wackherr and Home Prepared TiO$_2$-A comparative study. *Arab. J. Chem.* **2017**, *10*, S28–S34. [CrossRef]

13.  Liang, Y.; Guo, N.; Li, L.; Li, R.; Ji, G.; Gan, S. Fabrication of porous 3D flower-like Ag/ZnO heterostructure composites with enhanced photocatalytic performance. *Appl. Surf. Sci.* **2015**, *332*, 32–39. [CrossRef]

14.  Zhang, T.; Oyama, T.; Aoshima, A.; Hidaka, H.; Zhao, J. Serpone, hotooxidative N-demethylation of methylene blue in aqueous TiO$_2$ dispersions under UV irradiation. *J. Photochem. Photobiol. A Chem.* **2001**, *140*, 163–172. [CrossRef]

15.  Turchi, C.S.; Ollis, D.F. Photocatalytic degradation of organic water contaminants: Mechanisms involving hydroxyl radical attack. *J. Catal.* **1990**, *122*, 178–192. [CrossRef]

16.  Lee, K.M.; Lai, C.W.; Ngai, K.S.; Juan, J.C. Recent developments of zinc oxide based photocatalyst in water treatment technology: A review. *Water Res.* **2016**, *88*, 428–448. [CrossRef] [PubMed]

17.  Huang, S.T.; Jiang, Y.R.; Chou, S.Y.; Dai, Y.M.; Chen, C.C. Synthesis, characterization, photocatalytic activity of visible-light-responsive photocatalysts BiO$_x$Cl$_y$/BiO$_m$Br$_n$ by controlled hydrothermal method. *J. Mol. Catal. A Chem.* **2014**, *391*, 105–120. [CrossRef]

18.  Molla, M.A.I.; Tateishi, I.; Furukawa, M.; Katsumata, H.; Suzuki, T.; Kaneco, S. Evaluation of reaction mechanism for photocatalytic degradation of dye with self-sensitized TiO$_2$ under visible light irradiation. *Open J. Inorg. Non Met. Mater.* **2017**, *7*, 1–7.

19.  Park, H.; Park, Y.; Kim, W.; Choi, W. Surface modification of TiO$_2$ photocatalyst for environmental applications. *J. Photochem. Photobiol. C Photochem. Rev.* **2013**, *15*, 1–20. [CrossRef]

20.  Bessekhouad, Y.; Brahimi, R.; Hamdini, F.; Trari, M. Cu$_2$S/TiO$_2$ heterojunction applied to visible light Orange II degradation. *J. Photochem. Photobiol. A Chem.* **2012**, *248*, 15–23. [CrossRef]

21.  Prakash, O.; Kumar, S.; Singh, P.; Deckert, V.; Chatterjee, S.; Ghosh, A.K.; Singh, R.K. Surface-enhanced Raman scattering characteristics of CuO:Mn/Ag heterojunction probed by methyl orange: Effect of Mn$^{2+}$ doping. *J. Raman Spectrosc.* **2016**, *47*, 813–818. [CrossRef]

22.  Pan, L.; Zou, J.; Liu, X.; Liu, X.; Wang, S.; Zhang, X.; Wang, L. Visible-light-induced photodegradation of rhodamine B over hierarchical TiO$_2$: Effects of storage period and water-mediated adsorption switch. *Ind. Eng. Chem. Res.* **2012**, *51*, 12782–12786. [CrossRef]

23.  Su, Y.; Peng, L.; Guo, J.; Huang, S.; Lv, L.; Wang, X. Tunable optical and photocatalytic performance promoted by nonstoichiometric control and site-selective codoping of trivalent ions in NaTaO$_3$. *J. Phys. Chem. C* **2014**, *118*, 10728–10739. [CrossRef]

24. Fujishima, A.; Tao, T.N.; Tryk, D.A. Titanium dioxide photocatalysis. *J. Photochem. Photobiol. C Photochem. Rev.* **2000**, *1*, 1–21. [CrossRef]

25. Maa, J.; Wang, K.; Li, L.; Zhang, T.; Kong, Y.; Komarnenib, S. Visible-light photocatalytic decolorization of Orange II on $Cu_2O/ZnO$ nanocomposites. *Ceram. Int.* **2015**, *41*, 2050–2056. [CrossRef]

26. Vinodgopal, K.; Bedja, I.; Kamat, P.V. Nanostructured semiconductor films for photocatalysis. Photoelectrochemical behavior of $SnO_2/TiO_2$ composite systems and its role in photocatalytic degradation of a textile azo dye. *Chem. Mater.* **1996**, *8*, 2180–2187. [CrossRef]

27. Iliev, V. Phthalocyanine-modified titania-catalyst for photooxidation of phenols by irradiation with visible light. *J. Photochem. Photobiol. A Chem.* **2002**, *151*, 195–199. [CrossRef]

28. Turkten, N.; Cinar, Z. Photocatalytic decolorization of azo dyes on $TiO_2$: Prediction of mechanism via conceptual DFT. *Catal. Today* **2017**, *287*, 169–175. [CrossRef]

29. Konstantinou, I.K.; Albanis, T.A. $TiO_2$-assisted photocatalytic degradation of azo dyes in aqueous solution: Kinetic and mechanistic investigations. A review. *Appl. Catal. B Environ.* **2004**, *49*, 1–14. [CrossRef]

30. Xie, S.; Huang, P.; Kruzic, J.J.; Zeng, X.; Qian, H. A highly efficient degradation mechanism of methyl orange using Fe-based metallic glass powders. *Sci. Rep.* **2016**, *6*. [CrossRef] [PubMed]